

Hydrodynamics of domain walls in ferroelectrics and multiferroics: impact on memory devices

J. F. Scott, Donald M. Evans, J. M. Gregg, A. Gruverman

Angaben zur Veröffentlichung / Publication details:

Scott, J. F., Donald M. Evans, J. M. Gregg, and A. Gruverman. 2016. "Hydrodynamics of domain walls in ferroelectrics and multiferroics: impact on memory devices." *Applied Physics Letters* 109 (4): 042901. <https://doi.org/10.1063/1.4959996>.

Nutzungsbedingungen / Terms of use:

licgercopyright

Dieses Dokument wird unter folgenden Bedingungen zur Verfügung gestellt: / This document is made available under these conditions:

Deutsches Urheberrecht

Weitere Informationen finden Sie unter: / For more information see:

<https://www.uni-augsburg.de/de/organisation/bibliothek/publizieren-zitieren-archivieren/publiz/>



Hydrodynamics of domain walls in ferroelectrics and multiferroics: Impact on memory devices

Cite as: Appl. Phys. Lett. **109**, 042901 (2016); <https://doi.org/10.1063/1.4959996>

Submitted: 12 April 2016 • Accepted: 16 July 2016 • Published Online: 26 July 2016

 J. F. Scott, D. M. Evans, J. M. Gregg, et al.



View Online



Export Citation



CrossMark

ARTICLES YOU MAY BE INTERESTED IN

[Ferroelectric or non-ferroelectric: Why so many materials exhibit “ferroelectricity” on the nanoscale](#)

Applied Physics Reviews **4**, 021302 (2017); <https://doi.org/10.1063/1.4979015>

[Superdomain dynamics in ferroelectric-ferroelastic films: Switching, jamming, and relaxation](#)

Applied Physics Reviews **4**, 041104 (2017); <https://doi.org/10.1063/1.5005994>

[Ferroelectric thin films: Review of materials, properties, and applications](#)

Journal of Applied Physics **100**, 051606 (2006); <https://doi.org/10.1063/1.2336999>

 QBLOX



1 qubit

Shorten Setup Time

Auto-Calibration

More Qubits

Fully-integrated

Quantum Control Stacks

Ultrastable DC to 18.5 GHz

Synchronized <<1 ns

Ultralow noise



100s qubits

visit our website >

Hydrodynamics of domain walls in ferroelectrics and multiferroics: Impact on memory devices

J. F. Scott,¹ D. M. Evans,² J. M. Gregg,³ and A. Gruverman⁴

¹*School of Chemistry and School of Physics and Astronomy, St. Andrews University, St. Andrews, Scotland KY16 9ST, United Kingdom*

²*Earth Sciences Department, Cambridge University, Cambridge CB2 3EQ, United Kingdom*

³*School of Mathematics and Physics, Queen's University, Belfast, Northern Ireland BT7 1 NN, United Kingdom*

⁴*Department of Physics and Astronomy, University of Nebraska, Lincoln, Nebraska 68588, USA*

(Received 12 April 2016; accepted 16 July 2016; published online 26 July 2016)

The standard “Kittel Law” for the thickness and shape of ferroelectric, ferroelastic, or ferromagnet domains assumes mechanical equilibrium. The present paper shows that such domains may be highly nonequilibrium, with unusual thicknesses and shapes. In lead germanate and multiferroic lead zirconate titanate iron tantalate domain wall instabilities resemble hydrodynamics (Richtmyer–Meshkov and Helfrich–Hurault, respectively). *Published by AIP Publishing.* [<http://dx.doi.org/10.1063/1.4959996>]

Normally in ferroelectrics or ferroelastics the domains are rectilinear with straight edges, and the domain widths satisfy the Landau–Lifshitz–Kittel relationship (“Kittel Law”) as proportional to the square root of sample thickness. Here we present data on ferroelectric lead germanate and lead zirconate-titanate-iron-tantalate that exhibit curved circular or parabolic walls and violate the Kittel Law, demonstrating that they are nonequilibrium processes. These display similarities with the Richtmyer–Meshkov and Helfrich–Hurault instabilities in fluid mechanics and are good examples of the “domain glass” model of Salje and Carpenter. Their presence may be detrimental to multiferroic memory applications.

Very recently and very surprisingly the dynamics of electron transport in both graphene¹ and some low-temperature metals² have been shown to be dominated under some conditions by hydrodynamics. That is, electronic conduction is similar to fluid dynamics, with vortex motion, and not limited by Bloch theory. At about the same time it was shown^{3–5} that the ferroelastic domain walls in multiferroics⁶ are also controlled by fluid mechanics, with both wrinkling^{7–9} and folding^{3,4} at certain velocity thresholds, and hence that the domain walls may be treated as ballistic objects in high-viscosity media [n.b., wrinkling involves smoothly curved periodic modulation of domain walls, whereas folding consists of nearly 180° changes in direction]. In this sense semi-classical convection processes seem to appear in systems with very different basic dynamics.

The application of hydrodynamic models to domain walls in ferroelectrics is however not new. It was first used in detail¹⁰ by Dawber *et al.* in 2003. Their model is in turn based upon a full theory (cited) from the 1960s. The basic atomistic idea is that domain walls can be treated as ballistic objects in a viscous matrix. The domain wall viscosity arises in a pure material primarily from emission of acoustic phonon pairs. Using this model Dawber *et al.* matched not only the measured functional dependences (e.g., velocity versus applied electric field), but obtained quantitatively plausible numerical values, including 100 cm^{-1} for Brillouin zone boundary acoustic phonon energy. In its simplest form the model reduces to that of a bullet moving through a fluid.

The application of viscosity models to magnetic domains is even older; Skomski *et al.*¹¹ did that exactly twenty years ago. And this year Salje *et al.*^{12–14} found that ferroelastics are described well by hydrodynamics. The modest breakthrough in the present case follows the recent paper by Scott,³ which suggests that if indeed domain walls follow hydrodynamic flow, they should exhibit hydrodynamic instabilities also. And he showed rope-like folding instabilities. It is a modest paradigm shift to replace the equilibrium domain physics of the “Kittel Law” with these nonequilibrium dynamics.

In the present paper we examine data for two systems: Lead germanate, which importantly is *not* ferroelastic, which we examine on a mesoscopic domain scale (microns) and low-field scale; and lead zirconate-titanate iron tantalate, which is ferroelastic and which we examine on a nm-domain scale.

The wrinkling-folding instability critical field E_f is known to scale⁴ as the film thickness d as

$$E_f(d) = Ad^{4/9} \quad (1)$$

but this has not been tested for ferroelastic walls.

Richtmyer–Meshkov Instabilities: We note that the wrinkling of the $\text{Pb}_5\text{Ge}_3\text{O}_{11}$ domain wall in high applied electric fields E resembles the Richtmyer–Meshkov instability in adjacent fluid bilayers;^{16,17} here the field E is suddenly applied and initially produces small amplitude perturbations (wrinkling), which rapidly grow with time to a nonlinear regime (at a threshold of $E = 1$ or 2 kV/cm in lead germanate), resulting in bubble-like injection of spherical nanoferroelectric $+P$ domains into the $-P$ region (Figure 1); full scale of this figure is $380 \times 600\text{ }\mu\text{m}$. Note that the wavy wrinkles precede in time the nano-domain blobs. The ferroelectric region with polarization P parallel to E behaves as the lighter fluid in the Richtmyer–Meshkov model; if the vertical arrangement of the liquid bilayer is reversed, Meshkov found that needle-structures result, not spherical blobs (the plan view of these “spherical” blobs does not unambiguously reveal their shape in the direction normal to the surface—other geometries show that they are conical, not spherical).

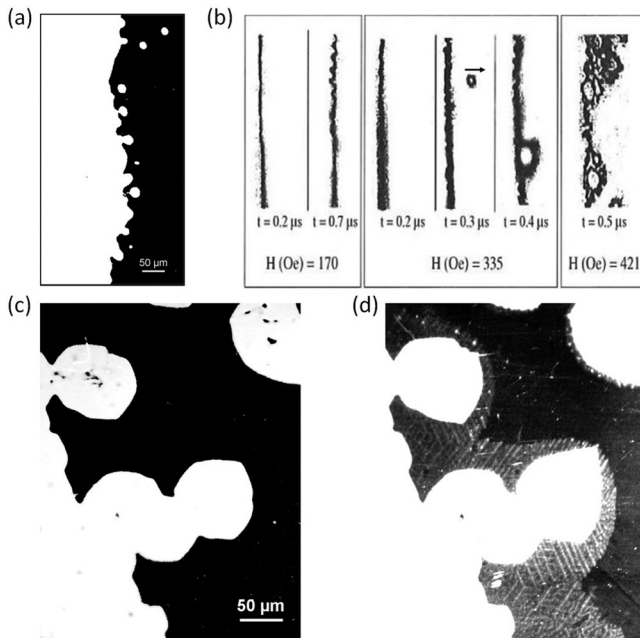


FIG. 1. (a). Emission of spherical ferroelectric nanodomains in lead germanate at ca. 1.5 kV cm^{-1} (full scale is ca. $380 \times 600 \mu\text{m}$) [this is an optical micrograph];^{7,8} (b) Emission of skyrmion-like magnetic nano-domains from a moving magnetic wall at different times and fields; modified from Randoshkin, with arrow showing direction of motion; see Ref. 20 for a matching skyrmion calculation. Not the wrinkling precursors at small fields and short times; (c) Skyrmion-like ferroelectric nano-domains^{7,8,27–31} being ejected upwards from an already wrinkled domain wall [see Ref. 3] by an applied electric field of ca. 2 kV/cm at ambient temperature in lead germanate $\text{Pb}_5\text{Ge}_3\text{O}_{11}$; these images are also optical. Note the longer wavelength wrinkling of the interface. Full width of figure is ca. $300 \mu\text{m}$. The lower (white) section is polarized upwards; the upper (black) section is polarized downwards. There is a similarity with the patterns of spherical ejections observed in Richtmyer–Meshkov instabilities^{10,11} in fluids subjected to nonlinear fields when the lower fluid is less dense than the upper one, whereas if the lower fluid is the denser, needle-like patterns are predicted. (d) Domain pattern for the same specimen in (a) but subjected to a square-wave voltage pulse sequence of $+2 \text{ kV/cm}$ and -2 kV/cm (left side—no voltage; right side, ac voltage train).

This asymmetry seems paradoxical; in fluids it arises from gravity, but in ferroelectrics it is not obvious and probably arises from subtle differences between top and bottom electrodes. The spherical shapes of the nano-domains in plan view in Figure 1 are not in themselves evidence of Richtmyer–Meshkov instabilities, since nano-domains are often spherical due to surface tension; in fact, other geometric views show that they are conical. The important point is that they are not needle-shaped.

Forward bias: The data for a positive field ($+V$ in Figure 1(a)) are compared with similar magnetic data, discussed further below, in Figure 1(b). The similarity is striking. There are three separate coercive fields in lead germanate: The lowest coercive field in lead germanate is about $0.5 = 1.0 \text{ kV/cm}$, a chain of domains appears at $3\text{--}6 \text{ kV/cm}$, non-through conical domains (broad domain boundary, e.g., BDB) forms at 7.5 kV/cm at a frequency of about 5 kHz . A specific shape of BDB depends on the pulse train parameters.

Reverse bias: In the Richtmyer–Meshkov model, reversing the direction of the applied force (voltage in our case) produces needle-like “domains” rather than spherical blobs. In Figures 1(c) and 1(d) we show the results of applying a pulse train of alternating $+V$ and $-V$ voltages, with E in each case ca. 1.5 kV/cm . This results in a superposition of needle-like

domains decorated with spherical nano-domains, supporting the prediction of the Richtmyer–Meshkov model. The direction of the needles is not random but favors specific crystallographic axes. In this sense the data differ from those in liquids.

There is also an analogy to voltage-induced crumpling in dielectric membranes, reported very recently.¹⁸ Crumpling is not an exact term but generally refers to stress-driven vertical wrinkles in a horizontal plate (often circular) with a threshold (see Ref. 13). The use of effective viscosity models is in general not new; it has been used for *magnetic* domains for twenty years.¹¹ In addition, the buckling of ferroelastic plates in a magnetic field has also been analyzed,¹⁹ along with a longer history of nonlinear bifurcations in ferroelastic martensitics²⁰ and ferroelectric films.

In the present work we extend this analysis to relate to quantitative measurements of domain wall velocities^{21–27} and effective masses for domain walls.

Helfrich–Hurault Mechanism: In contrast to the discussion above of wrinkling and Richtmyer–Meshkov instabilities in ferroelectric lead germanate, which occur only in high fields E , and where the ferroic walls are ferroelectric but not ferroelastic, another instability, a purely ferroelastic one, occurs in lead iron tantalate zirconate-titanate at zero electric field but nonzero applied stress; in this system the ferroelectric walls are not coincident with the ferroelastic ones, but lie inside them.

Figure 2 illustrates some unpublished data from Ref. 28. The smallest domains are rectangular ferroelectric domains ca. 5 nm wide which are inside larger (ca. 100-nm) ferroelastic domains. The latter have curved walls.

Our hypothesis is that the ferroelastic walls result from domain motion in a viscous medium (damping is provided by acoustic phonons).¹⁰ Although this provides a plausible explanation for the curved walls, as shown in Figure 2 below, we emphasize that we have no temporal information to support this dynamical model. Hence it is possible that the curvature shown in Figures 1 and 2 arises from some purely electrostatic mechanism.

However, in support of the hydrodynamic viscosity model, we have compatible data and modeling from Salje.^{5,12–15}

Salje’s Model: The basic assumption in Salje’s model is that unlike ferroelectric switching, the hysteresis in ferroelastic switching is dominated by continuum fluid mechanics

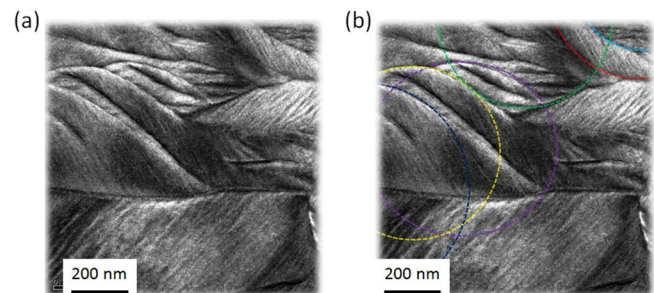


FIG. 2. TEM micrograph of lead-iron-tantalate-zirconate-titanate.²³ The ferroelectric domains are black and white stripes ca. 5 nm wide with straight edges, inside at ca. 45° with respect to the walls of the larger ferroelastic domains with curved sides. White spot is Ga-ion implantation from the FIB process. Circular curves fitted as aids to the eye. Note that the radii of curvature vary considerably, probably ruling out effects of underlying carbon grids.

and not the lattice symmetry. He points out that for the strain reversal step from $-S$ to $+S$, under a positive (reversing) stress to an initially negative strain, the ferroelastic hysteresis is dominated by viscous flow, with a complex domain structure sometimes describable as a “domain glass.”

By comparison the step from $+S(0)$ to $+S(\text{stress})$ is not hydrodynamic, but proceeds via conventional dynamics and often involves needle-like propagating domains.

Open-channel Viscous Flow: Another model we consider here is the open channel viscous flow. This is motivated by the curved front such mechanisms produce (Figure 3). It is qualitatively different from the Helfrich–Hurault model above in an important way: It has no velocity threshold. We do not present it here as an alternative to Helfrich–Hurault instability, but rather as a possible low-velocity precursor to the latter, at velocities below the folding threshold.

We need to relate the figures above in terms of channel width w , film thickness or depth d , velocity maximum $v(m)$, and some sort of Reynolds number. We can use the creep velocity $v = 1 \text{ nms}^{-1}$ from Tybell *et al.*,²³ see also more recently Ng, Ahluwalia *et al.*^{24–26} and Scott and Kumar.²⁵ The effective mass for the wall is ca. one proton mass m_p .²⁷ The basic idea is that relatively low-viscosity media produce folds, whereas higher viscosity media produce skyrmions and vortex structures.^{28–31} The vortex structures (and skyrmions^{32–35}) are analogous to high viscosity aa-aa lava, just as the smooth folds are analogous to those in lower viscosity ropy pahoehoe. Note also that folding is known to be created via focused ion beams (FIB) in polymers,³² and the samples in Ref. 16, including Figure 3 above, were all subject to FIB.

We know a few useful parameters from other work: The average domain wall velocity at low fields in perovskite oxides is ca. 1 nms^{-1} .^{24–30} The ferroelastic domain wall viscosity is very large compared with normal liquids, and comparable with that in martensitic metals; a rough estimate by Scott³ is 10^6 poise for domain wall viscosity and by Salje and Carpenter³² is 10^{13} poise for a structural glass. The typical ratio of radius of curvature to domain in-plane width is ca. 15:1 to 20:1 for the large domains (shaped like grapefruit segments). (The larger the radius of curvature, the larger the shear modulus required for the instability threshold.⁴⁵) These parameters may be helpful for future modeling but are insufficient to determine effective Rayleigh or Reynolds numbers.

Parabolic Shapes for Ferroelastic Domain Wall: One way to compare data with Helfrich–Hurault boundaries and the shape of open-channel steady-state flow in Figure 3 is the exact shape: Both Helfrich–Hurault boundaries and steady-state fronts are expected to be parabolic, although steady-state fronts

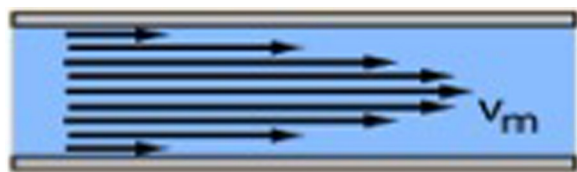


FIG. 3. Schematic model of velocity distribution in open-channel viscous flow. This is to be compared with the curved ferroelastic walls in Figure 2. Note that velocity goes to zero at the edges, giving straight edges, as in Figure 2 far from the apparent vertex of each wall; this is a deviation from exactly parabolic.

should have infinite slopes exactly at the boundaries or pinning sites, where non-slip boundary conditions give zero velocity (Figure 3).

Possible artifacts: It is always useful to play Devil’s Advocate with one’s own data. So we ask whether the TEM data above could arise from the underlying carbon grid in the system. Such grids consist of a connected set of disk-shaped carbon, with radii of curvature similar to those of the larger arcs marked in Figure 2. However, the data shown in Figure 2(a) (marked) have various different radii of curvature, from $\gg 1 \mu\text{m}$ to a little greater than 200 nm, which is not compatible with the carbon grids used; and the high degree of overlap in Figure 2(b) makes carbon grids highly unlikely. Moreover, our samples are probably too thick (80–100 nm) for carbon grids to be seen through them via TEM. But we do not see identical patterns via atomic force microscopy (AFM/piezo-force microscopy (PFM)) on samples with no TEM carbon grids. The folding of domains may arise from the FIB process; and at least some of the parabolic domain wall shapes may be influenced by the carbon grid in the TEM microscopy. However, we emphasize that the radii of curvature for the ferroelastic domains vary considerably and overlap greatly, which is incompatible with a carbon grid TEM pattern but suggestive of Helfrich–Hurault flow.

Summary and Models (Richtmyer–Meshkov and Helfrich–Hurault): The observation of nonlinear instabilities for wrinkling and emission of spherical nano-domains in ferroelectrics has previously been described successfully by skyrmion models. However, in the present work we broaden that description to make contact with other nonlinear models from fluid mechanics. Evidence for folding in ferroelastic thin films is presented and related to studies on other materials. Such phenomena seem to be rather generic in physics, ranging from gold films^{36,37} to lava.³⁸ The use of hydrodynamic models in ferroic crystals for elastic domain wall dynamics is however rather new, and the key idea involved for multiferroic PFTZT is that ferroelectric nano-domains lie within ferroelastic micro-domains.³⁹ This description is qualitatively different from the equilibrium minimum-energy ferroelastic wall model of Roitburd,⁴⁰ which is based upon the magnetic domain model of Landau–Lifshitz–Kittel (frequently termed the Kittel Law); the latter models assume infinite lateral dimensions and no folding. They are models based upon minimizing energies at or near equilibrium, not local nonlinear forces. As discussed recently, our preferred models are not close to equilibrium nor small perturbations: Even the old (1943) Ramsberg–Osgood model is of the form $F = -kx + bx^2 + cx^n$, where $n = \text{ca. } 5$ and $cx^n \gg b$, not $\ll b$. This is not a weak anharmonic perturbation.

There is an extensive literature in the field of liquid crystals on electro-hydrodynamic models, beginning with Gleeson.⁴¹ And in addition to the Richtmyer–Meshkov model mentioned above for lead germanate, there is a close analogy for PFTZT with the Helfrich–Hurault layer-instability in liquid crystals.^{42–44} This is a sliding lamellar instability in smectic liquid crystals, characterized, as with the present data, by crescent-shaped domains. Unfortunately,⁴⁵ no comprehensive theory for such nonlinear irreversible processes exists, nor can the fluctuation-dissipation theorem be used. However, following De Gennes, the critical field E_c for folding can be

estimated as $\epsilon_0 \epsilon_a E(\text{crit})^2 = 2\pi K/(Ld)$, where L is a length scale equal to the square root of the ratio of shear modulus K to bulk modulus B , and d is a wrinkling length scale of order $100\text{ }\mu\text{m}$ in smectics. This typically gives for smectics with roughly $K = 2\text{ pN}$ and $B = 50\text{ MNm}^{-2}$, $E_c = \text{ca. } 200\text{ kV/cm} = 20\text{ MV/m}$, which is much larger than the wrinkling threshold in Fig. 1 for ferroelectric walls in lead germanate of ca. 2 kV cm^{-1} . It is important to note that the shapes of domains with these lamellar instabilities is parabolic,⁴⁶ similar to that in Figure 2. The similarity of the present layer-instabilities in ferroelastic films and Helfrich–Hurault models should be investigated further. Nonlinear folding in viscous sheets has been studied without simple solutions for more than a century, so one should not underestimate the problem. Recently this task has been taken up by many authors, and theory and experiment for fold sizes are given elsewhere.^{47–49} Generally, the fold size L varies as the inverse square root of viscosity. For filamentary bifurcations (e.g., honey poured on bread)

$$L = h(4\rho g/3\mu v r^2)^{1/4}, \quad (2)$$

where ρ is density; g , gravitational acceleration; μ , viscosity (10 Pa); r , radius of filament (1 mm); v , velocity (0.1 ms^{-1}); and h , height of fall (0.1 m). For honey this gives macroscopic fold lengths ca. a few mm. But for our ferroelastic domain walls, with $v = 1\text{ nms}^{-1}$ (10^8 smaller), viscosity 10^6 times larger, and small h , this predicts micron or submicron fold lengths.

It is appropriate to ask why lead germanate does not exhibit the folding instabilities seen in PFTZT. A possible answer is that the ferroelectric transition in lead germanate is not ferroelastic: It is from trigonal C3 point group to trigonal C3h. Generally, to be ferroelastic it is necessary and sufficient for a transition to change crystal class.⁵⁰ Hence $\text{Pb}_5\text{Ge}_3\text{O}_{11}$ cannot exhibit ferroelastic domains.

Implications for Memory Devices: Ferroelectric memories are already in high-volume production ($\$100$ million/year) level as commercial devices for transit fare cards and cash machines. The chips are produced by Samsung and packaged in Korea and Japan under several brand names, e.g., Suica or Felica for fare cards and Edy for cash machines (“e-money”). The active ferroelectric material is also ferroelastic. If these memories are to widen their applications to faster devices, then higher fields will be required (same voltage but thinner films). At present, such devices typically run at 5 V across 100 nm (50 kV cm^{-1}); hence the instability here near a few kV cm^{-1} is below present norms. At such fields the ferroelastic wall instability thresholds discussed here may serve as the rate-limiting parameters.

We should carry out additional experiments to determine if the circular domain wall patterning arises during growth, switching, or the FIB processing, or the electron microscopy. However, the present experiments are very difficult. First, a ceramic of good quality (single-phase) must be produced. Then, because we cannot have grain boundaries in these domain wall studies, a single crystal of submicron dimensions must be cut out via FIB. Then we must carry out TEM studies (and usually AFM/PFM) on these submicron specimens.

- ¹I. Torre, A. Tomadin, A. K. Geim, and M. Polini, *Phys. Rev. B* **92**, 165433 (2015).
- ²P. J. W. Moll, P. Kushwaha, N. Nandi, B. Schmidt, and A. P. Mackenzie, *Science* **351**, 1061 (2016).
- ³J. F. Scott, *J. Phys.: Condens. Matter* **27**, 492001 (2015).
- ⁴D. P. Holmes and A. J. Crosby, *Phys. Rev. Lett.* **105**, 038303 (2010).
- ⁵E. K.-H. Salje, paper presented at Workshop on Oxides, Cargese, Corsica (2015).
- ⁶D. M. Evans, A. Schilling, A. Kumar, D. Sanchez, N. Ortega, M. Arrondondo, R. Katiyar, J. M. Gregg, and J. F. Scott, *Nat. Commun.* **4**, 1534 (2013).
- ⁷M. Dawber, D. J. Jung, and J. F. Scott, *Appl. Phys. Lett.* **82**, 436 (2003).
- ⁸A. Gruverman, Ph.D. thesis, Ural State University, Ekaterinburg, USSR, 1990.
- ⁹V. Ya. Shur, A. L. Gruverman, V. V. Letuchev, E. L. Rumyantsev, and A. L. Subbotin, “Domain structure of lead germanate,” *Ferroelectrics* **98**, 29 (1989).
- ¹⁰M. Dawber, A. Gruverman, and J. F. Scott, *J. Phys.: Condens. Matter* **18**, L71 (2006).
- ¹¹R. Skomski, J. Giergiel, and J. Kirschner, *IEEE Trans. Mag.* **32**, 4576 (1996).
- ¹²E. Salje and M. A. Carpenter, *Phys. Status Solidi B* **252**, 2639 (2015).
- ¹³B. Houchmandzadeh, J. Lajzerowicz, and E. Salje, *Phase Trans. A* **38**, 77 (1992).
- ¹⁴H. Poettker and E. Salje, *J. Phys.: Condens. Matter* **28**, 075902 (2016).
- ¹⁵D. Viehland and E. K. H. Salje, *Adv. Phys.* **63**, 267 (2014).
- ¹⁶D. Richtmyer, *Commun. Pure Appl. Math.* **13**, 297 (1960).
- ¹⁷E. E. Meshkov, *Sov. Fluid Dyn.* **4**, 101 (1969).
- ¹⁸B. Li, X. Liu, L. Liu, and H. Chen, *Eur. Phys. Lett.* **112**, 56004 (2015).
- ¹⁹H. King, R. D. Schroll, B. Davidovitch, and N. Menon, *Proc. Nat. Acad. Sci.* **109**, 9716 (2012).
- ²⁰F. Moon, *J. Appl. Mech.* **37**, 153 (1970).
- ²¹J. Pouget, *Phase Trans.* **34**, 105 (1991).
- ²²K. Lee and S. Baik, *Ann. Rev. Mater. Res.* **36**, 81 (2006).
- ²³T. Tybell, P. Paruch, and J.-M. Triscone, *Phys. Rev. Lett.* **89**, 097601 (2002).
- ²⁴N. Ng, R. Ahluwalia, A. Kumar, D. J. Srolovitz, P. Chandra, and J. F. Scott, *Appl. Phys. Lett.* **107**, 152902 (2015).
- ²⁵J. F. Scott and A. Kumar, *Appl. Phys. Lett.* **105**, 052902 (2014).
- ²⁶R. Ahluwalia, N. Ng, A. Schilling, R. McQuaid, D. M. Evans, J. M. Gregg, D. Srolovitz, and J. F. Scott, *Phys. Rev. Lett.* **111**, 165702 (2013).
- ²⁷F. Kagawa, N. Minami, S. Horiuchi, and Y. Tokura, *Nat. Commun.* **7**, 10675 (2016).
- ²⁸D. M. Evans, Ph.D. thesis, Queens University, Belfast, 2013.
- ²⁹V. Nagarajan, A. Roytburd, A. Stanishevsky, S. Prasertchoung, T. Zhao, L. Chen, J. Melngailis, O. Auciello, and R. Ramesh, *Nat. Mater.* **2**, 43 (2003).
- ³⁰A. K. Yadav, C. T. Nelson, S. L. Hsu, Z. Hong, J. D. Clarkson, C. M. Schlepuezt, A. R. Damodaran, P. Shafer, E. Arenholz, L. R. Dedon *et al.*, *Nature* **530**, 198 (2016).
- ³¹J. Pouget and G. A. Maugin, *Phys. Rev. B* **30**, 5306 (1984).
- ³²V. V. Randoshkin, *Fiz. Tverd. Tela* **37**, 355 (1995), [*Sov. Phys.–Solid State* **65**, 152 (1995)].
- ³³A. Kudryavtsev, B. M. A. G. Piette, and W. J. Zakrzewski, *Nonlinearity* **11**, 783 (1998).
- ³⁴A. Kudryavtsev, B. M. A. G. Piette, and W. J. Zakrzewski, *Phys. Rev. D* **61**, 025016 (2000).
- ³⁵A. Kudryavtsev, B. M. A. G. Piette, and W. J. Zakrzewski, *Eur. Phys. J. C* **1**, 333 (1998).
- ³⁶M.-W. Moon, S.-H. Lee, J.-Y. Sun, K.-H. Oh, A. Vaziri, and J. W. Hutchinson, *Proc. Nat. Acad. Sci.* **104**, 1130 (2006).
- ³⁷J. Colin, C. Coupeau, and J. Grilhe, *Phys. Rev. Lett.* **99**, 046101 (2007).
- ³⁸J. H. Fink and R. C. Fletcher, *J. Volcanol. Geotherm. Res.* **4**, 151 (1978).
- ³⁹V. Janovec and J. Privratska, *International Meeting Ferroelectrics (IMF)*, Krakow (2013), p. 517.
- ⁴⁰A. L. Roitburd, *Phys. Status Solidi A* **37**, 329 (1976).
- ⁴¹J. T. Gleeson, *Nature* **385**, 511 (1997).
- ⁴²W. Helfrich, *Phys. Rev. Lett.* **23**, 372 (1969).
- ⁴³J. P. Hurault, *J. Chem. Phys.* **59**, 2068 (1973).
- ⁴⁴G. Napoli and A. Nobili, *Phys. Rev. E* **80**, 031710 (2009).
- ⁴⁵O. V. Manyuhina and M. J. Bowick, *Int. J. Nonlinear Mech.* **75**, 87 (2015).
- ⁴⁶A. E. H. Love, *Phil. Trans. R. Soc. A* **179**, 491 (1888).
- ⁴⁷B. I. Senyuk, I. I. Smalyukh, and O. D. Lavrentovich, *Phys. Rev. E* **74**, 011712 (2006).
- ⁴⁸M. Skorobogatiy and L. Mahadevan, *Eur. Phys. Lett.* **52**, 532 (2000).
- ⁴⁹E. Cerda, K. Ravi-Chandar, and L. Mahadevan, *Nature* **419**, 579 (2002).
- ⁵⁰J.-C. Toledano, *Ann. Telecommun.* **29**, 249 (1974).